Loss Calculation and Thermal Analysis of Axial AMB in HTR-PM Helium Circulator

Haoyu Zuo [1,2,3], Zhengang Shi [1,2,3], Yangbo Zheng [1,2,3], Jinpeng Yu [1,2,3], Tianpeng Fan [1,2,3], and Ni Mo [*1,2,3]

[1] Institute of Nuclear and New Energy Technology
Tsinghua University, Beijing 100084, China

[2] Collaborative Innovation Center of Advanced Nuclear Energy Technology
Tsinghua University, Beijing 100084, China

[3] The Key Laboratory of Advanced Reactor Engineering and Safety
Ministry of Education, Beijing, 100084, China
zuohy16@mails.tsinghua.edu.cn, moni@tsinghua.edu.cn*

Abstract **─** The helium circulator is one of the important components of the High Temperature Gas-cooled Reactor Pebble Bed Module (HTR-PM). It uses the electromagnetic suspension technology to support the rotor, the so-called magnetic bearing technology. Considering the performance and safety issues on the axial active magnetic bearing(AMB) caused by potential high temperature, this paper calculates copper loss, iron loss and wind loss in axial AMB and simulates temperature field under a normal operating condition, and compares the results with the experimental data.

Index Terms **─** Axial magnetic bearing, copper loss, helium circulator, iron loss, temperature field, wind loss.

I. INTRODUCTION

The HTR-PM is one of the most promising candidates for the next generation reactors. It's renowned for its inherent safety, system simplification and high power generation efficiency.

The helium circulator is the key equipment in the primary loop of the HTR-PM and installed at the output at the steam generator. It drives helium coolant with an average temperature of 750℃ to circulate in the primary loop for heat exchange released by the nuclear reaction [1]. Figure 1 shows a cross section of the HTR-PM reactor.

The rotor of helium circulator is supported by axial active magnetic bearings (AMB) instead of mechanical bearings for its excellent performance of non-contact, non-polluting and high-speed characteristics [2]. But there still exist copper loss, iron loss and wind loss in magnetic bearings, leading to an increase in temperature and affecting the performance of the AMB system under some special conditions. Therefore, it is necessary to calculate the losses and the temperature field of the axial AMB in HTR-PM.

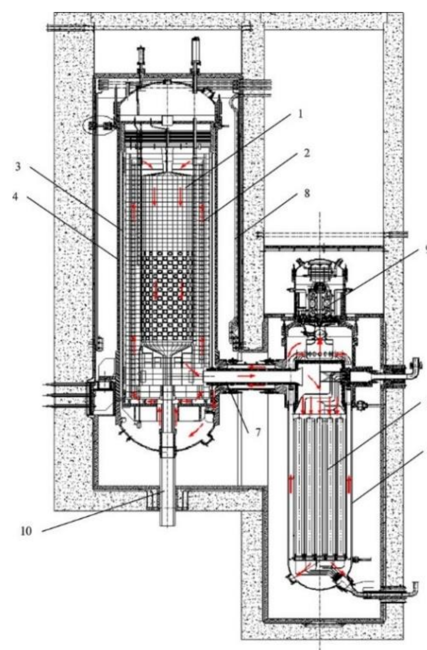

Fig. 1. Cross section of the primary loop of the HTR-PM (1. reactor core; 2. side reflector and carbon thermal shield; 3. core barrel; 4. reactor pressure vessel; 5. steam generator; 6. steam generator vessel; 7. coaxial gas duct; 8. water-cooling panel; 9. blower; 10. fuel discharging tube).

Submitted On: June 29, 2018
Accepted On: October 1, 2018

Researches have been done including theoretical and experimental studies on iron loss of laminated magnets: Karsarda proposed the calculation formulas for eddy current and hysteresis loss of laminated magnets [3-4]; Marinescu [5] discussed the possibility of calculating the eddy current loss of permanent magnet bearings in two dimensions. For solid axial bearings with a single-coil structure, Sun [6-7] proposed analytical solutions and finite element solutions for eddy current losses considering electromagnet temperature coupling.

As for the research of AMB temperature field, Sun [6-7] solved the temperature field while neglecting the wind loss and considering eddy current losses as an even distributed internal heat source in the mathematical model of the temperature field.

In this paper, based on the actual operation current data of the HTR-PM axial AMB, the losses of the axial bearing are studied. Furthermore, the temperature field is modeled and theoretically analyzed on ANSYS platform. The theoretical simulation analysis results are compared with the actual temperature data. The simulation results are in accordance with the actual operating data, which provides a theoretical model support and an effective calculation method for the subsequent optimization design of the axial AMB.

II. GEOMETRIC MODEL OF AXIAL AMB IN HTR-PM

The HTR-PM axial bearing is used to support the gravity of the rotor in the helium circulator. The rotor has a length of 3.3 meters and a mass of 4000 kg. The speed at normal operation is 4000 r/min. The structure of axial magnetic bearing is shown in Fig. 2, including 4 main sections: thrust disk, stators, coils and rotor. The parameter is shown in Table 1.

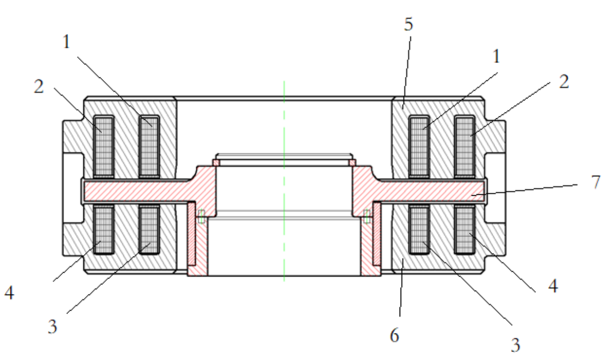

Fig. 2. Structure of the axial AMB (1. upper stator inner coil; 2. upper stator outer coil; 3. lower stator inner coil; 4. lower stator outer coil; 5. upper stator; 6. lower stator; 7. thrust disk).

Table 1: Parameters of the axial AMB

Parameter	Unit	Value
Gap between stator and rotor	mm	1
Inner magnetic pole area, A_i	mm^2	7868.8
Central magnetic pole area, A_c	mm^2	15009.2
Outer magnetic pole area, A_o	mm^2	9982.1
Trust disk diameter	mm	300
Vacuum permeability, $\mu 0$	N/A^2	$4\pi\times10\text{-}7\approx 1.256637\times10\text{-}6$
Winding turns	-	78, 78

The actual HTR-PM axial bearing structure is complex. In order to save computing resources, the geometric model used in this paper simplifies the connecting nuts between the components, the chamfers, and the disassembly tooling of the thrust disk, and the windings are processed solidly. The model is shown in Fig. 3 below. The following three assumptions are the bases for the loss calculation and temperature field analysis:

(1) The eddy current has the same effect on each strand of the axial AMB, and the loss is evenly distributed on the wingdings;

(2) The temperature difference inside the bearing is not large and the radiation is neglected;

(3) The actual solid surface is ideally flat and the thermal contact resistance is ignored.

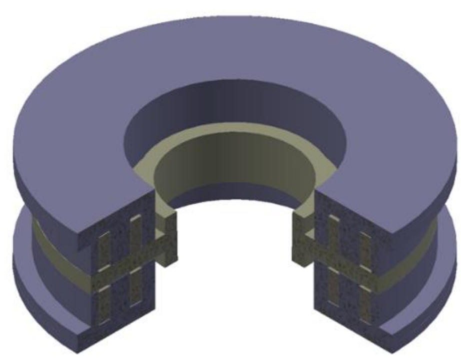

Fig. 3. Geometric model of axial AMB.

III. LOSSES CALCULATION

While the axial AMB realizes the stable support of the rotor in HTR-PM, the winding needs a large current to generate the electromagnetic force that balances the gravity and aerodynamic force of the rotor, and there will also be current fluctuations in the actual operation. During high-speed rotating, there will be copper loss and iron loss in the stator and thrust disk, and wind loss on the surface of the thrust disk. Based on the actual operating condition and current data, the copper loss, iron loss, and wind loss of the axial AMB are analyzed.

A. Operating condition

Excluding start, shutdown and some special abnormal conditions, the HTR-PM helium circulator are usually in normal operating conditions, the following analysis and calculation are based on this condition. The operating parameters of the HTR-PM helium circulator are shown in Table 2.

Table 2: Main operating parameters of helium circulator

Parameter	Unit	Value
Medium	-	Helium
Rated speed	r/min	4000
Mass flow	kg/s	96
Inlet pressure	Mpa	7
Speed range	%	20~105
Medium density	kg/m3	6.33
Circulator chamber ambient temperature	°C	65

B. Copper loss

The gravitational force and aerodynamic force of the rotor are balanced by the electromagnetic force generated by the winding's current. The loss caused by the current passing through the winding is called the copper loss. The actual electrical parameters of the upper and lower coils are measured at 25°C and the results are shown in Table 3, and the copper loss of the axial bearings can be calculated by formula (1):

$$P_{\mathrm{Cu}} = Ri^2 \,. \tag{1}$$

Among them, P_{cu} is the copper loss of axial bearings in W, R is the resistance of the winding in Ω, i is the current in A.

Table 3: Resistance of axial AMB

Parameters	Unit	Value
Upper winding inner coil resistance	Ω	0.38
Upper winding outer coil resistance	Ω	0.37
Lower winding inner coil resistance	Ω	0.38
Lower winding outer coil resistance	Ω	0.37

The measured average value of the upper and lower winding currents under normal operation is 36.5A and 23.7A respectively. Through the calculation of formula (1), the copper loss during normal operation are shown in Table 4.

Table 4: Copper losses of axial AMB

Parameters	Unit	Value
Upper stator inner coil copper loss	W	506
Upper stator outer coil copper loss	W	492
Lower stator inner coil copper loss	W	213
Lower stator outer coil copper loss	W	207

C. Iron loss

The classic theory of iron loss point that iron loss can be divided into eddy current loss, hysteresis loss and other losses. Eddy current loss is the energy loss caused by the induced current generated in the conductor when it moves in a non-uniform magnetic field or is in a time-varying magnetic field. Hysteresis loss refers to the energy consumed by the hysteresis of the ferromagnetic magnet during repetitive magnetization.

Iron loss mainly exists in the stator and thrust disks of the axial AMB, which material is 40CrNiMoA soft magnetic material. Because of manufacturing processes and other reasons, axial AMB are made in solid structure, for which means the eddy current loss is relatively large compared with the hysteresis loss. Therefore, only the eddy current losses are considered in the calculation of iron loss, which can be described by equation (2):

$$p_{iron} = p_{eddy}(x, y, z) \,. \tag{2}$$

Among them, P_{iron} is the iron loss of axial bearings in W, P_{eddy} is the eddy current loss of axial bearings in W.

In order to accurately calculate the three-dimensional distribution of the eddy current loss in the solid double-coil axial AMB, the actual speed and the current data are obtained from actual parameters under normal operating conditions as the bases of calculation.

The Fourier-transformation of the upper and lower axial bearing current data in the running state is performed, and the main frequency is extracted. The results are shown in Fig. 4 and Fig. 5, which show the actual current of the axial bearing has a significant dominant frequency of 56 Hz.

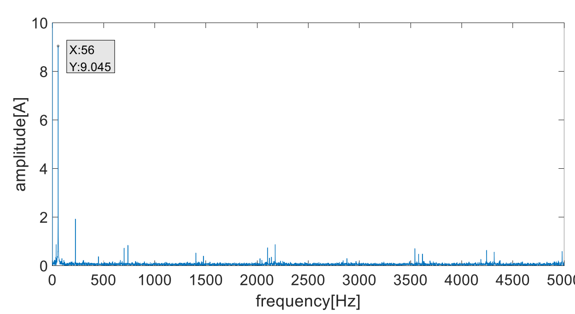

Fig. 4. Fourier Transform of upper axial AMB current.

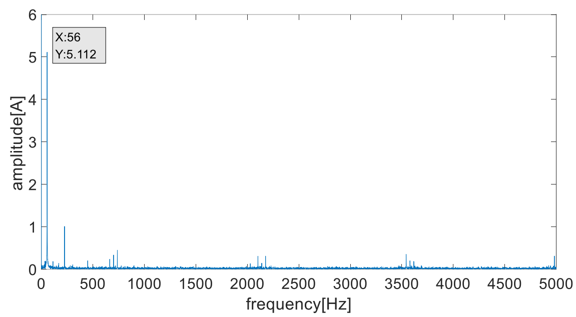

Fig. 5. Fourier Transform of lower axial AMB current.

The fitting current function and the comparison between fitting current and the actual current are shown in Table 5, Fig. 6 and Fig. 7.

Table 5: Fitted currents

Current	Fitting Function
Upper axial AMB current	$I = 36.64 + 8.18\cos 352.2t - 18.55\sin 352.2t$
Lower axial AMB current	$I = 23.74 - 5.37\cos 353.4t - 10.13\sin 353.4t$

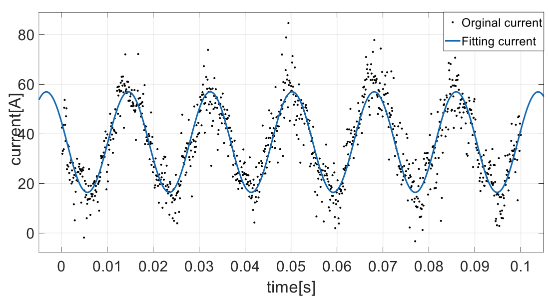

Fig. 6. Upper fitted current curve and original current.

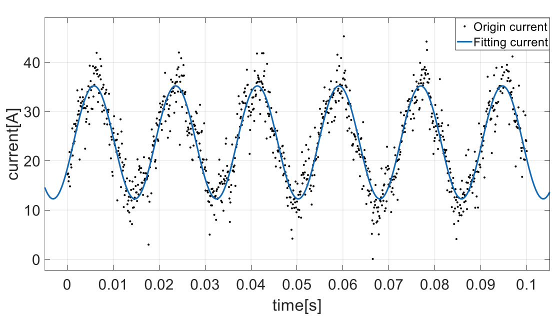

Fig. 7. Lower fitted current curve and original current.

The eddy current loss distribution of the stator and thrust disk is obtained by the finite element method. The results are shown in in Fig. 8 to Fig. 10, the eddy current loss is concentrated around the windings in the stator and concentrated on the corresponding positions of the windings on the thrust disk.

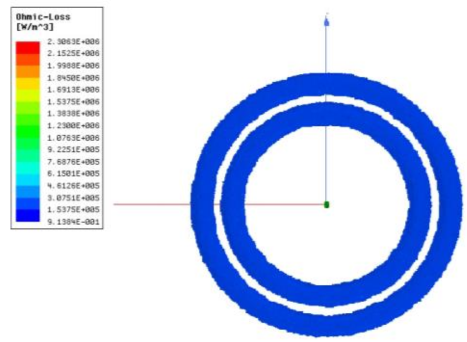

Fig. 8. Eddy current loss distribution in upper stator.

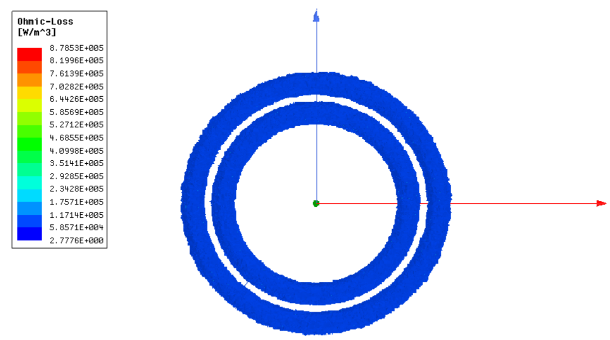

Fig. 9. Eddy current loss distribution in lower stator.

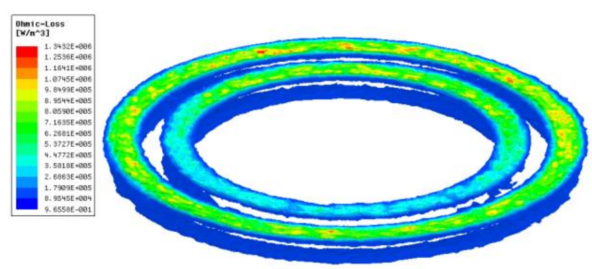

Fig. 10. Eddy current loss distribution in thrust disk.

The eddy current loss in each part is calculated as Table 6:

Table 6: Eddy current loss calculation

Part	Unit	Eddy Current Loss
Upper stator	W	2622
Lower stator	W	787
Thrust disk	W	559

D. Wind loss

As shown in Fig. 1, the high-speed rotating thrust disk is supported by the axial AMB, so there is a forced flow of gas in the air gap. The friction generated between the gas and the rotor is wind loss. Wind losses mainly exist on the disk surfaces and end surfaces of high-speed rotating thrust disks. The wind loss is not related to the electrical parameters of the axial AMB, the calculation of the wind loss can refer to the research of the rotating machine.

End-face wind loss can be based on the empirical formula of Von Karman's plate turbulence model as formula (3):

$$P_w = [0.074\rho_g L\pi R^4 \left(\frac{v}{2\pi R^2}\right)^{0.2}]\omega^{2.8}. \tag{3}$$

Among them, ρ_g is the density of the gas in kg/m^3, ν is the kinematic viscosity of the gas in m^2/s, R is the radius of the thrust disk in m, L is the length of thrust disk in m, ω is the rotational angular velocity in rad/s.

For the disc surface, the formula for different flow patterns are proposed by Etemad [8], the formula (4) is based on the turbulence model:

$$P_w = 0.311\left(\frac{s}{r}\right)^{-1/4}\mu^{1/4}\rho^{3/4}\omega^{11/4}r^{9/2}. \tag{4}$$

Among them, s is the air gap width in m, r is the radium of the disk in m, and μ is the dynamic viscosity of the gas in Pa·s. The calculation is measured on one side.

The parameter for wind loss calculation and results are shown in Table 7 and Table 8.

Table 7: Parameter for wind loss calculation

Parameters	Unit	Value
Ambient helium temperature	°C	65
Helium pressure	MPa	7
Helium density	kg/m^3	9.686420455
Helium dynamic viscosity	Pa·s	2.1592×10-5
Helium kinematic viscosity	m^2/s	2.2291×10-6
Radium of thrust disk, r	mm	300
Length of thrust disk, L	mm	32
Air gap width	mm	0.8
Rotational angular velocity	rad/s	418.67

Table 8: Wind loss results

Parameters	Unit	Value
Wind loss on end surface	W	1673
Wind loss on one disk surface	W	2089

E. Results analysis

Through calculation and analysis of the copper loss, iron loss and wind loss of the HTR-PM helium circulator axial AMB under normal operating conditions, the results are shown in Table 9. The total loss in the axial bearing is 9446W, among which the wind loss accounted for the largest proportion, followed by the proportion of iron loss, and the copper loss accounted for the smallest proportion. The results are in good agreement with the actual project conditions.

Table 9: Percentage of each loss

Loss	Unit	Value	Percentage
Iron loss	W	3968	42.0%
Copper loss	W	1418	15.0%
Wind loss	W	4060	43.0%
Total loss	W	9446	100%

IV. TEMPERATURE FIELD ANALYSIS AND CALCULATION

Based on the results of the losses of the axial bearings in the HTR-PM helium circulator, the mathematical model of temperature field is established for the analysis.

A. Mathematical model of temperature field

According to the law of Fourier heat conduction, the three-dimensional steady-state temperature field of an axial AMB can be described as a differential conduction equation in Cartesian coordinates, as shown in equation (5):

$$\rho C_p \frac{\partial T}{\partial t} = \lambda\left(\frac{\partial^2 T}{\partial x^2} + \frac{\partial^2 T}{\partial y^2} + \frac{\partial^2 T}{\partial z^2}\right) + p_v. \tag{5}$$

Among them, ρ is the density in kg/m^3, C_p is the constant-pressure specific heat in J/(kg·K), λ is the thermal conductivity in W/(m·K), P_v is the inner heat source in W/m^3.

The eddy current loss is unevenly distributed, and the copper loss is evenly distributed in the conductors formed by each strand:

$$p_v = p_{eddy}(x, y, z) + p_{copper}. \tag{6}$$

The boundary conditions for the mathematical model of the temperature field include fixed heat flux and convection heat transfer boundaries:

$$q_s = const, \tag{7}$$

$$-\lambda\frac{\partial T}{\partial n} = h(T_w - T_f)\cdot \tag{8}$$

Among them, q_s is the fixed heat flux, h is the convective heat transfer coefficient.

The fixed heat flux q_s is equal to the wind loss q_w caused by the rotation in formula (3) and (4), and the convection heat transfer coefficient in formula (8) is calculated by the corresponding correlation [9].

B. Results and analysis

The temperature field results shown in Figs. 11 to 13 are obtained by solving equation (1)-(8) by the ANSYS under normal operating condition.

The temperature of the upper axial AMB is shown in the Fig. 11: axially, the temperature of the upper axial bearing increases from the surface close to the thrust disk to the surface far away from the thrust disk, because the high speed rotating causes a large forced convective heat transfer coefficient; radially, there are relatively high temperature areas at the tooth between the two slots and outer coil, because copper loss and eddy current loss are concentrated in this location. The maximum temperature of the upper axial bearing is 75.42°C.

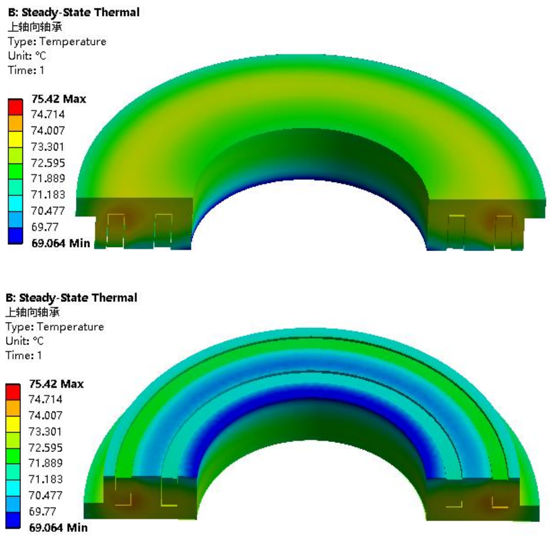

Fig. 11. Temperature field of upper Axial AMB.

The temperature field of the lower axial AMB is shown in the Fig. 12: the lower axial bearing have a similar temperature gradient distribution with the upper axial bearing. Because the lower axial bearing generates less copper loss and iron loss compared to the upper one, the temperature is slightly lower and the maximum temperature of the lower axial bearing is 71.56°C.

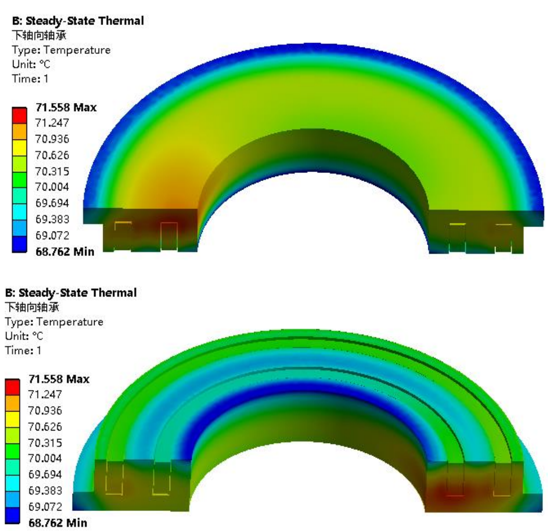

Fig. 12. Temperature field of lower Axial AMB.

The temperature field of the thrust disk is shown in the Fig. 13. The average temperature of the upper surface of the thrust plate is higher than the lower surface, and due to the distribution of iron loss on the surface of the thrust plate, there are obvious high temperature areas on the upper and lower surfaces of the thrust disk. The high temperature areas are mainly concentrated on the thrust disk surface facing the coils on the stator, which is about 2°C higher than the average temperature on the surface. The maximum temperature of the thrust disk is 75.46°C.

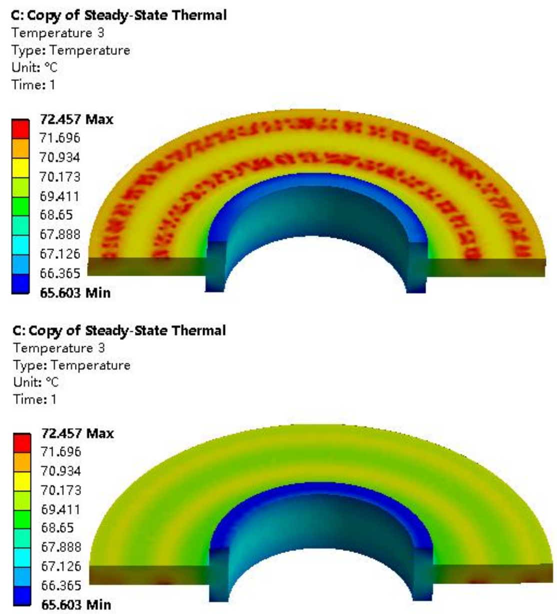

Fig. 13. Temperature field of thrust disk.

Four test points are arranged near the inner and outer coils of the upper and lower axial AMB of the helium circulator, and the speed of the rotor during experiment is 3710r/min.

The test point temperature under the test condition and the maximum temperature in the calculation are shown in Table 10, both are below the allowable temperature limitation 150°C.

Table 10: Comparison of simulation and experimental results

Measuring Point	Experiment Results/°C	Calculation Results/°C (Maximum)	Relative Error/%
Upper axial AMB inner coil temperature	85.0	75.4	-11.08%
Upper axial AMB outer coil temperature	82.6	74.0	-10.41%

There is certain error between the experimental results and the calculation results. The main reasons for the are as follows:

(1) Windings are affected by factors such as the outsourcing insulating varnish, and the actual windings are different from solid copper which assumed in this article.

(2) When considering the copper loss, the effect of temperature increase on the resistance is ignored.

(3) The corresponding convective heat transfer coefficient at a specific location is inconsistent with the actual situation. Therefore, the calculation results will deviate from the actual situation.

V. CONCLUSION

(1) The article calculates the loss of the axial AMB of the HTR-PM helium circulator under the normal operating condition. The results show that there are concentrated areas of eddy current loss on the stator and the thrust disk, and the wind loss of the axial AMB can't be ignored.

(2) In this paper, ANSYS is used to calculate the steady-state temperature field of the axial AMB in HTR-PM helium circulator under normal operation, the results show that the temperature is below the allowable temperature limitation. Comparing with the results of field tests, the calculated results are basically consistent with the experimental results, which show the correctness of the model and method, and thus can provide a reliable basis for the design of an axial AMB in helium circulation.

(3) From the simulation results, it can be seen that the upper stator temperature is higher than the lower stator temperature, the temperature is higher in the area where iron loss concentrates inside the axial bearing stator. There is also a higher temperature area where the iron loss concentrates on the surface of the thrust disk.

ACKNOWLEDGMENT

This paper is financially supported by the National Science and technology major projects (ZX 06901) and 61305065 by NSFC.

REFERENCES

[1] Y. Zheng, J. Lapins, E. Laurien, L. Shi, and Z. Zhang, "Thermal hydraulic analysis of a pebble-bed modular high temperature gas-cooled reactor with attica3d and thermix codes," *Nuclear Engineering and Design*, 246 (2012/05/01/2012): 286-97.

[2] G. Yang, S. Zhengang, and Ni Mo, "Technical design and engineering prototype experiment of active magnetic bearing for helium blower of Htr-Pm," *Annals of Nuclear Energy*, 71 (2014/09/01/2014): 103-10.

[3] M. E. F. Kasarda, P. E. Allaire, E. H. Maslen, et al., "High-speed rotor losses in a radial eight-pole magnetic bearing: Part 1-Experimental measurement," *ASME J. Eng. Gas Turbines Power*, vol. 120, pp. 110-114, Jan. 1998.

[4] M. E. F. Kasarda, P. E. Allaire, E. H. Maslen, et al., "High-speed rotor losses in a radial eight-pole magnetic bearing: Part 2-Analytical/empirical models and calculations," *ASME J. Eng. Gas Turbines Power*, vol. 120, pp. 110-114, Jan. 1998.

[5] M. Marinescu, N. Marinescu, and W. Bernreuther, "A 2-D treatment of the eddy currents induced by transversal oscillations of permanent magnet rings in conducting axisymmetric plates," *IEEE Transactions on Magnetics*, vol. 28, no. 2, pp. 1386-89, 1992.

[6] S. Shouqun, G. Haipeng, and G Keqian, 'Transient temperature field in active thrust magnetic bearing," *Chinese Journal of Mechanical Engineering*, no. 04, pp. 575-78, 2005.

[7] S. Shouquan and Z. Guoquan, "Analysis of eddy current loss inthrust magnetic bearing considering electormagento temperature coupling," *University of Shanghai for Science and Technology*, no. 03, pp. 194-97+202, 2005. (In Chinese).

[8] M. R. Etemad, K. Pullen, C. B. Besant, et al., "Evaluation of windage losses for high-speed disc machinery," *Proc. Instn. Mech. Engrs.*, vol. 206, pp. 149-157, 1992.

[9] I. Shevchuk, "Convective heat and mass transfer in rotating disk systems," vol. 45, 2009. doi:10.1007/978-3-642-00718-7.

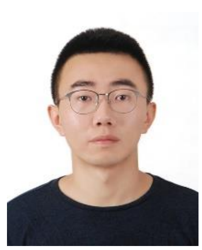

Haoyu Zuo graduated from Power Engineering Department of North China Electric Power University, and now is a second year Master candidate in Institute of Nuclear and New Energy Technology of Tsinghua University. His main research is loss calculation and temperature analysis in helium circulator.

Zhengang Shi received his Ph.D. in Nuclear Science & Technology at Tsinghua University in 2003. He is now working at Institute of Nuclear and New Energy Technology, Tsinghua University, Beijing, China. Shi's research subject is magnetic bearing.